Am J Transl Res 2023;15(7):4454-4466
www.ajtr.org /ISSN:1943-8141/AJTR0149427

Original Article

iTRAQ-based proteomic analysis of imiquimod in the treatment of ulcerative colitis

Jinkun Guo[1*], Na Chen[1*], Feifei Tan[1], Julan Zhou[1], Hongyu Xiang[1], Yu Luo[2], Zhongyin Zhou[1]

[1]Department of Gastroenterology, Renmin Hospital of Wuhan University, Hubei Key Laboratory of Digestive System Disease, Wuhan 430060, Hubei, China; [2]Jingmen Hospital of Traditional Chinese Medicine, Jingmen 448001, Hubei, China. [*]Equal contributors and co-first authors.

Received January 31, 2023; Accepted June 7, 2023; Epub July 15, 2023; Published July 30, 2023

Abstract: Objective: In this study, we explored the potential mechanisms and the signaling pathways involved in the treatment of Ulcerative Colitis (UC) with imiquimod (IMQ). Methods: The UC mouse model was established by treating C57BL/6J mice with 3% Dextran Sulfate Sodium (DSS). Then, the UC-related symptoms were examined. Disease Activity Index (DAI) was estimated based on weight loss, stool consistency, and occult bleeding or hematochezia. Histological changes were evaluated by Hematoxylin and Eosin (H&E) staining. Furthermore, we used multiplexed Isobaric Tagging for Relative and Absolute Protein Quantification (iTRAQ) technique coupled with high-throughput liquid chromatography tandem mass spectrometry (LC-MS/MS) to determine the differentially expressed proteins (DEPs). Results: Administration of 3% DSS for 7 days induced acute colitis associated with diarrhea, hematochezia, weight loss, and colon shortening. However, after IMQ administration, almost all the above symptoms were improved by different degrees. Specifically, the DAI, histological disorder, and colon shortening were attenuated. In iTRAQ analysis, a total of 4170 proteins were identified with a high confidence (≥ 95% confidence). The numbers of DEPs between the normal and UC model mice, between the normal and the IMQ-treated therapy mice, as well as between the model and the therapy mice were 317, 253, and 209, respectively. Gene Ontology (GO) and Kyoto Encyclopedia of Genes and Genomes (KEGG) analyses revealed that the DEPs involved in the complement and coagulation cascades were downregulated in IMQ-treated therapy group. Conclusions: IMQ might ameliorate colitis by suppressing the complement and coagulation cascades pathway, which might serve as new therapeutic strategies for the treatment of patients with UC.

Keywords: iTRAQ, imiquimod, proteomics, ulcerative colitis, differentially expressed proteins

Introduction

Ulcerative Colitis (UC) is a chronic non-specific inflammatory disease in the colon that is characterized by alternating relapsing and remitting mucosal inflammation, which starts at the rectum and extends to the proximal colon [1]. In recent years, the incidence and prevalence of UC are increasing worldwide [2], and the patients with prolonged UC have an increased risk for colorectal cancer [3]. However, the etiology and pathogenesis of UC remain to be defined due to its heterogeneity. Accumulating evidence has indicated the association of UC with immune system disorders, genetic factors, environmental factors, and microbial infection [4, 5]. Although many drugs are available to treat UC, most of them only relieve symptoms without a radical cure. Therefore, it is urgent to develop more effective drugs for the treatment of UC.

Imiquimod (IMQ), a member of imidazoquinolines family, is an immune response modifier that acts as a Toll-like receptor 7 agonist [6]. Several studies have suggested that IMQ can stimulate the innate and adaptive immune responses as well as induce cytokine production. Because of its antiviral, anti-tumor and immunoregulatory effects, IMQ has been widely used in in vitro and in vivo studies as well as tested in clinical trials, such as dermatology trials [7, 8]. However, IMQ in the treatment of UC is rarely reported.

Table 1. Assessment of the DAI

DAI score	Weight loss (%)	Stool consistency	Occult/gross bleeding
0	None	Normal	Normal
1	1-5		
2	5-10	Loose stools	Hemoccult positive
3	10-20		
4	> 20	Diarrhea	Gross bleeding

DAI, disease activity index.

Multiplexed Isobaric Tagging for Relative and Absolute Protein Quantification (iTRAQ) coupled with liquid chromatography tandem mass spectrometry (LC-MS/MS) has been one of the most popular methods for quantitative proteomics and has been employed in various areas as the advent of new proteomic techniques [9]. iTRAQ is suitable to all kinds of samples, and up to 8 samples can be analyzed simultaneously by commercially available kits. In addition, iTRAQ is superior to traditional techniques with high sensitivity, high throughput, and high stability [10, 11].

In this study, iTRAQ-coupled LC-MS/MS was used to identify the differentially expressed proteins (DEPs) that were related to the therapeutic effect of IMQ in the mouse model of UC. Furthermore, bioinformatics analysis was performed to annotate the protein function and to elucidate the mechanism underlying the therapeutic effect of IMQ. Hence, our findings shed light on the application of IMQ in the treatment of UC.

Materials and methods

Animals

Eight-week-old wild-type male C57BL/6J mice (18-22 g body weight) were purchased from Vital River Laboratory Animal Technology Co., Ltd. (certificate No. 32002100001086). Mice were housed in an SPF facility at the experimental animal center of Renmin Hospital of Wuhan University (certificate No. SYXK(E) 2019-0027) and acclimatized under standard conditions with a 12/12 h day/night cycle and free access to chow and water for a week before being used in an experiment. All animal experiments were performed strictly according to the China legislation regarding the use and care of laboratory animals and approved by the Wuhan University Animal Care Committee.

Drugs and reagents

Dextran sulfate sodium (DSS; molecular mass, 36-50 kDa) and Imiquimod (IMQ) were purchased from MP Biomedicals (Santa Ana, CA, USA) and TCI Development Co, Ltd. (Shanghai, China), respectively. The fecal occult blood test kit was obtained from Baso Bio Co., LTD. (Zhuhai, China). Paraformaldehyde and trypsin were obtained from GeneCreate Biological Engineering Co., Ltd. (Wuhan, China).

Experimental design

After 7 days of acclimatization, sixty mice were randomly divided into normal control (designated as Normal), UC model (Model), and IMQ-treated therapy (Therapy) groups (n=20 per group). Mice the in Model and Therapy groups were fed with 3% DSS-containing drinking water for 7 consecutive days ad libitum to induce colitis. During the study period, mice in the Therapy group received a single oral gavage of IMQ (30 mg/kg of body weigh) daily. An equal volume of sterile PBS was administrated to the Normal and the Model groups. The body weight, stool consistency, and hematochezia of mice were monitored daily to evaluate the Disease Activity Index (DAI). At day 8, mice were sacrificed by cervical dislocation, and the colons were dissected for further analysis. First, the length of colons was measured. Then, a part of the distal colon was fixed in 4% paraformaldehyde for Hematoxylin and Eosin (H&E) staining, while the rest was frozen in liquid nitrogen and stored at -80°C for proteomic analysis.

DAI assessment

The DAI was assessed by weight loss, stool consistency, and occult bleeding or hematochezia according to the scoring system (**Table 1**) [12]. The DAI was calculated as the sum of these three scores.

Histopathological assessment

Briefly, colon tissues were dissected, fixed, dehydrated in xylene, embedded in paraffin, and sectioned for H&E staining. The degree of colon injury was assessed by histopathology examinations on the infiltration of inflammatory cells, the depth of the lesions, and the destruction degree of the crypt structure. The level of

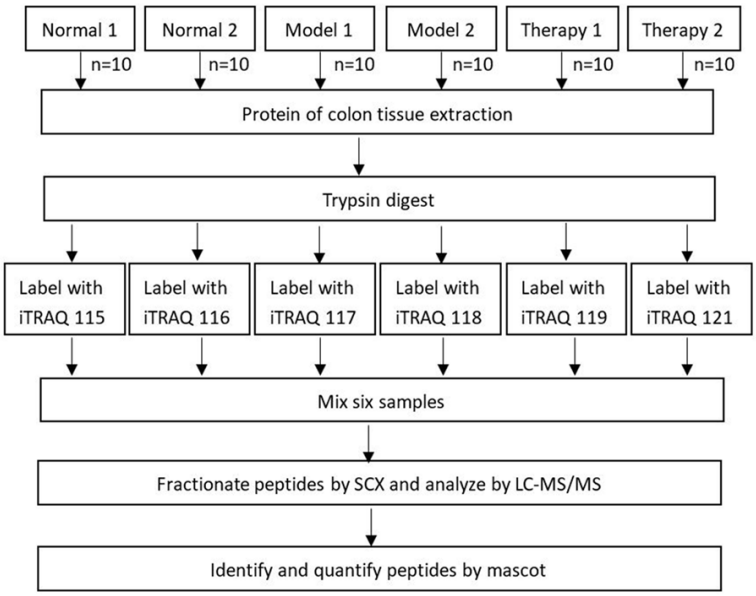

Figure 1. The workflow of the iTRAQ-based proteomic analysis. iTRAQ, Isobaric Tagging for Relative and Absolute Protein Quantification. LC-MS/MS, liquid chromatography tandem mass spectrometry.

disease was graded according to the scoring system described by Dieleman et al. [13].

iTRAQ proteomics analysis

To prepare samples for iTRAQ proteomics analysis, the twenty colon tissues from each group (Normal, Model, and Therapy) were randomly divided into two subgroups (n=10 per group), namely Normal 1 and 2, Model 1 and 2, and Therapy 1 and 2. Thus, each sample was a pool of ten tissues, and samples from each group had two biological repeats.

The proteins from these 6 samples were extracted using the acetone method [14] and quantified using the Bradford method [15]. Then, 100 μg of protein was reduced, alkylated, and digested with trypsin overnight at 37°C, followed by labeling with iTRAQ Reagent-8 plex Multiplex Kit (AB Sciex U.K. Limited) according to the manufacture's protocol. Briefly, the 6 samples were labeled with the iTRAQ tags as the Normal (115 and 116 tags), Model (117 and 118 tags), and Therapy (119 and 121 tags) groups. Equal amount from each labeled sample was mixed and fractionated by high performance liquid chromatography (HPLC) system (Thermo DINOEX Ultimate 3000 BioRS) using a Durashell C18 (5be, 100 Å, 4.6×250 mm). At the end, 12 fractions were collected and dried in a vacuum concentrator. Subsequently, LC-MS/MS analysis was performed on the AB SCIEX nanoLC-MS/MS (Triple TOF 5600 plus) system. The workflow of the iTRAQ-based proteomic analysis is shown in **Figure 1**.

Bioinformatics analysis

The original MS/MS data were submitted to ProteinPilot Software version 4.5 (AB SCIEX) for data analysis. Only proteins with at least one unique peptide and unused value of more than 1.3 were extracted for further analysis. A ratio of ≥ 1.5 or ≤ 0.67 and *p*-value ≤ 0.05 were considered differentially expressed. To predict the functions of the identified proteins, the identified protein sequences were blasted with Gene Ontology (GO) Terms (http://geneontology.org/), including biological process, cellular component, and molecular function. In addition, Kyoto Encyclopedia of Genes and Genomes (KEGG) pathway (http://www.kegg.jp/kegg/pathway.html) analysis was also performed to determine pathway enrichment. Clusters of Orthologous Groups of Proteins System (COG, http://www.ncbi.nlm.nih.gov/COG/) was used for the functional annotation of genes from new genomes and to study the genome evolution.

Statistical analysis

All statistical analysis was performed using SPSS 25.0 software. The data were presented as the mean ± standard deviation (SD). Comparison among groups was conducted by one-way analysis of variance (ANOVA), while Student's t tests were used for comparison between groups. *P*-value < 0.05 was considered statistically significant.

Results

The effects of IMQ on DSS-induced colitis

In this study, treating mice with DSS successfully induced acute UC, as indicated by the obvious diarrhea, hematochezia, weight loss, which

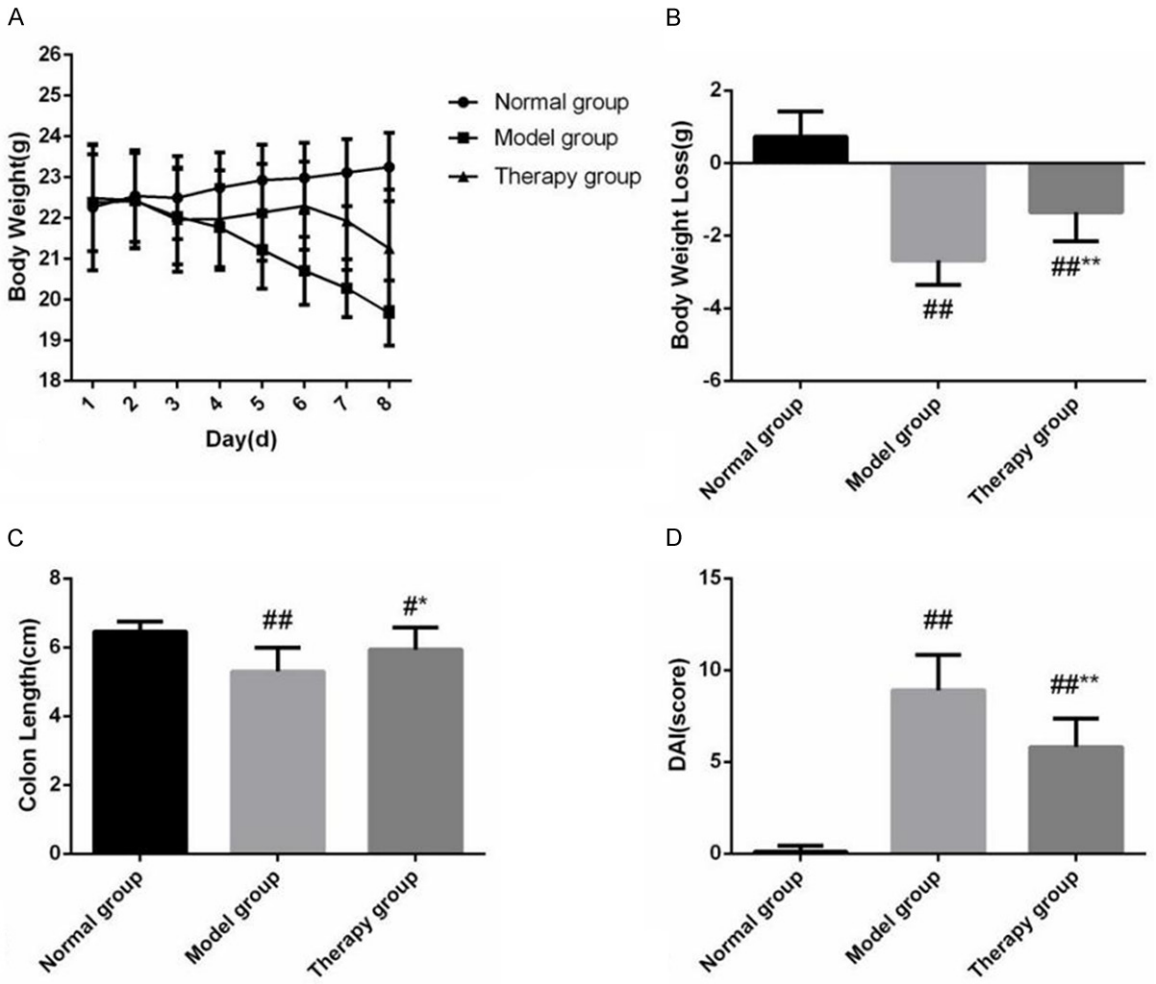

Figure 2. IMQ attenuated DSS-induced colitis. A. Body weight was measured daily. B. Body weight. C. Colon length. D. DAI score of mice in each group was measured. Data are presented as mean ± S.D. (n=20). $^{\#}P < 0.05$, $^{\#\#}P < 0.01$ vs Normal group, $^{*}P < 0.05$, $^{**}P < 0.01$ vs Model group. IMQ, imiquimod. DSS, Dextran Sulfate Sodium. DAI, disease activity index.

could be ameliorated by IMQ treatment. Specifically, while the body weight of mice in the Model group was significantly decreased (**Figure 2A** and **2B**) compared to the control mice ($P < 0.01$), IMQ treatment increased their body weight ($P < 0.01$). Similarly, although the colon length of mice in the Model group was significantly shorter (**Figure 2C**) compared to control mice ($P < 0.01$), IMQ could attenuate this effect ($P < 0.05$). In addition, the mice in the Model group had a significantly increased DAI score (**Figure 2D**) which was decrease in IMQ-treated mice ($P < 0.01$).

IMQ ameliorates histological damage in DSS-induced colitis

As shown in **Figure 3A**, the control mice exhibited an intact colon structure. In contrast, the mice in the Model group displayed a disordered colon structure with a loss of colonic epithelial cells, mucosal ulcerations, the destruction of crypt architecture, and an extensive inflammatory cell infiltration (**Figure 3B**). However, IMQ treatment alleviated these symptoms (**Figure 3C**) and decreased the histological scores ($P < 0.01$) (**Figure 3D**).

Protein identification and quantification by iTRAQ analysis

To explore the mechanism of IMQ function, we carried out a global profiling of quantitative proteome on the mice of the Normal, Model, and Therapy groups and identified 4170 proteins from 22,897 distinct peptides derived from 126,498 spectra with a high confidence (≥ 95% confidence) and unique peptide matches ≥ 1

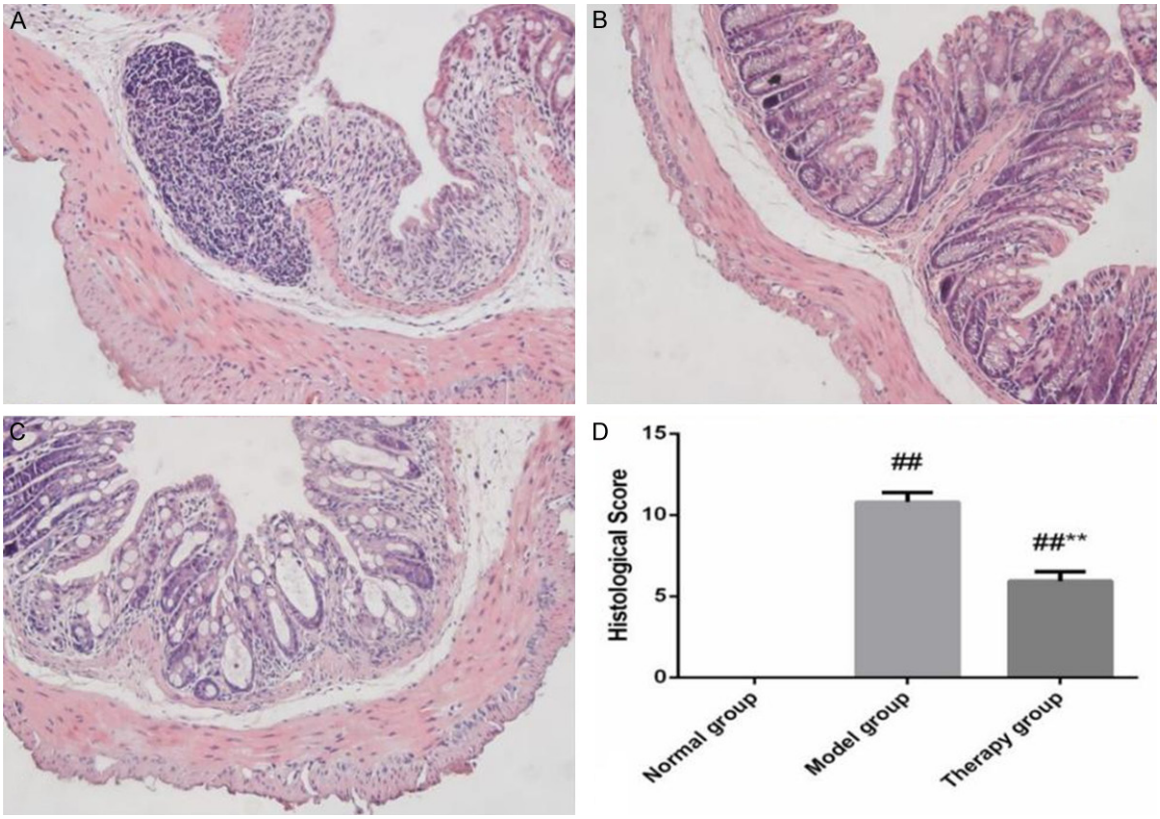

Figure 3. IMQ alleviated colon damage in mice with DSS-induced colitis. A-C. H&E staining of colonic tissues. Magnification ×200. D. Histological scores of the colonic tissue in three groups. Data are presented as mean ± S.D. (n=20). $^{\#}P < 0.05$, $^{\#\#}P < 0.01$ vs Normal group, $^{*}P < 0.05$, $^{**}P < 0.01$ vs Model group. IMQ, imiquimod. DSS, Dextran Sulfate Sodium.

Table 2. Assessment of DEPs (P ≤ 0.05)

Sample pairs	Normal vs Model	Normal vs Therapy	Model vs Therapy
Quantified	4019	4033	4030
Upregulated	156	114	81
Downregulated	161	139	128
Total DEPs	317	253	209

DEPs, differentially expressed proteins.

using iTRAQ coupled with LC-MS/MS. Among them, 4019, 4033, and 4030 proteins were identified in the Normal, Model, and Therapy groups, respectively. Using fold changes ≥ 1.5 or ≤ 0.67 with *p*-value ≤ 0.05 as cutoff, 317 DEPs including 156 upregulated and 161 downregulated proteins were identified between the Normal and Model groups, while 253 DEPs (114 were obtained between the control and IMQ-treatment mice) of which 114 proteins were upregulated and the 139 proteins were downregulated. Comparison between UC and IMQ-treatment mice identified 209 with 81

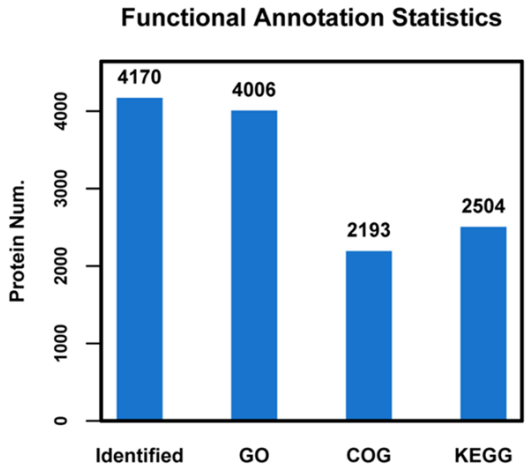

Figure 4. Histogram of different functional annotations. X-axis represented different annotation databases, and Y-axis represented protein number. GO, Gene Ontology. COG, Clusters of Orthologous Groups. KEGG, Kyoto Encyclopedia of Genes and Genomes.

upregulated and 128 downregulated proteins (**Table 2**).

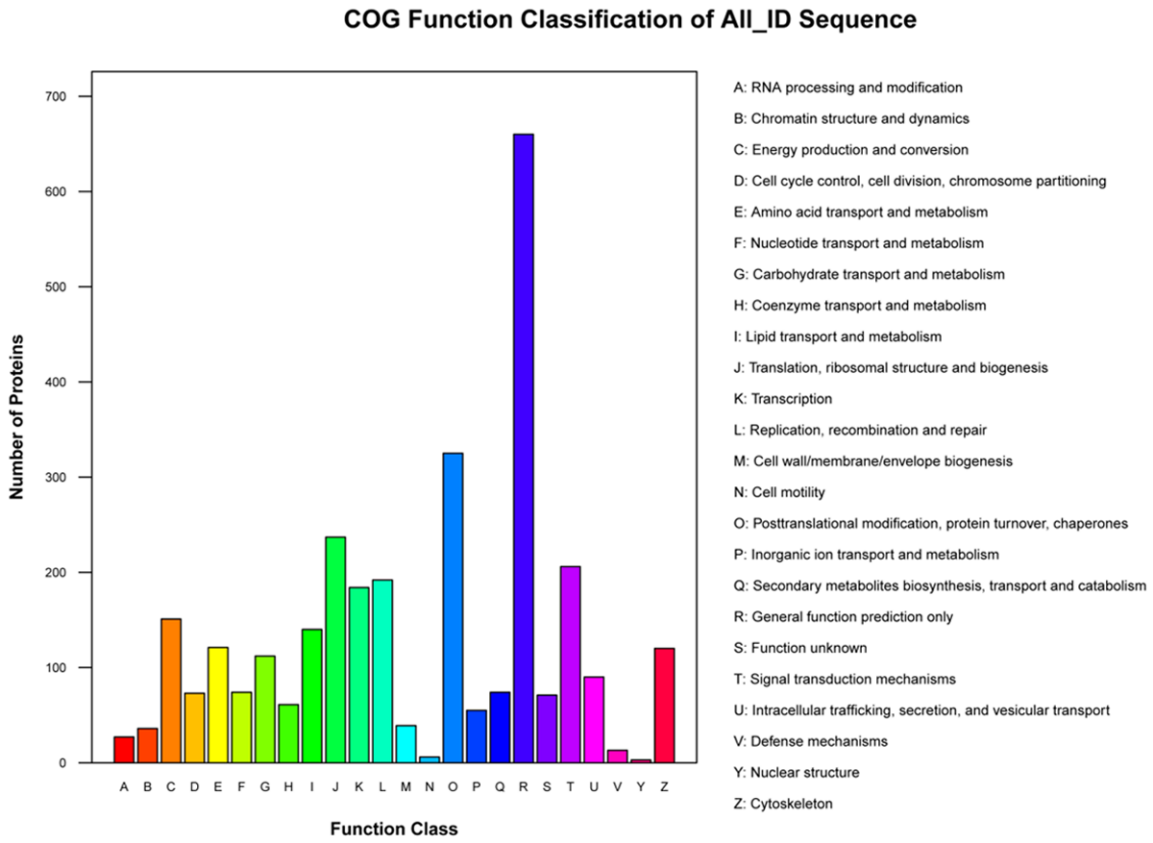

Figure 5. Functional classifications of identified proteins into COG groups. The x-axis represented different classifications, and the y-axis represented the number of proteins in each COG class. COG, Clusters of Orthologous Groups.

Functional annotations of identified proteins

To understand the functional significance of the 4170 proteins identified by iTRAQ coupled with LC-MS/MS, we performed GO and KEGG using the database of different sources as shown in **Figure 4**, among the 4170 proteins, 4006 proteins were sub-categorized into 58 classifications by GO annotation, including 28 biological process, 12 cellular component, and 18 molecular function, while 2193 proteins were sub-categorized into 24 COG classifications, and the R (General function prediction only) was the most highly represented (**Figure 5**). In addition, 2504 proteins were sub-categorized into 152 KEGG classifications. The GO annotation was performed with blast2go v4.5 pipeline, and we found the proteins were enriched in cellular process (12.50%), followed by metabolic process (10.82%) and biological regulation (8.46%) (**Figure 6A**). Furthermore, for the cellular component analysis, these proteins were enriched in cell (18.98%), followed by cell part (18.95%) and organelle (12.73%) (**Figure 6B**). Notably, the top enriched molecular functions were binding (51.34%), catalytic activity (27.41%), and enzyme regulator activity (5.17%) (**Figure 6C**).

Bioinformatic analysis of the DEPs

To further assess the function of DEPs, we independently annotated and analyzed the upregulated and downregulated DEPs from different groups of mice. The DEPs between Normal and Model groups were classified into 48 functional categories, including 26 biological processes, 10 cellular components, and 12 molecular functions. (**Figure 7A**), while the DEPs between Model and Therapy groups were assigned to 50 categories including 26 biological processes, 12 cellular components, and 12 molecular functions (**Figure 7B**). In addition, the DEPs between the Normal and the Therapy groups were enriched in 51 categories, including 25 biological processes, 12 cellular compo-

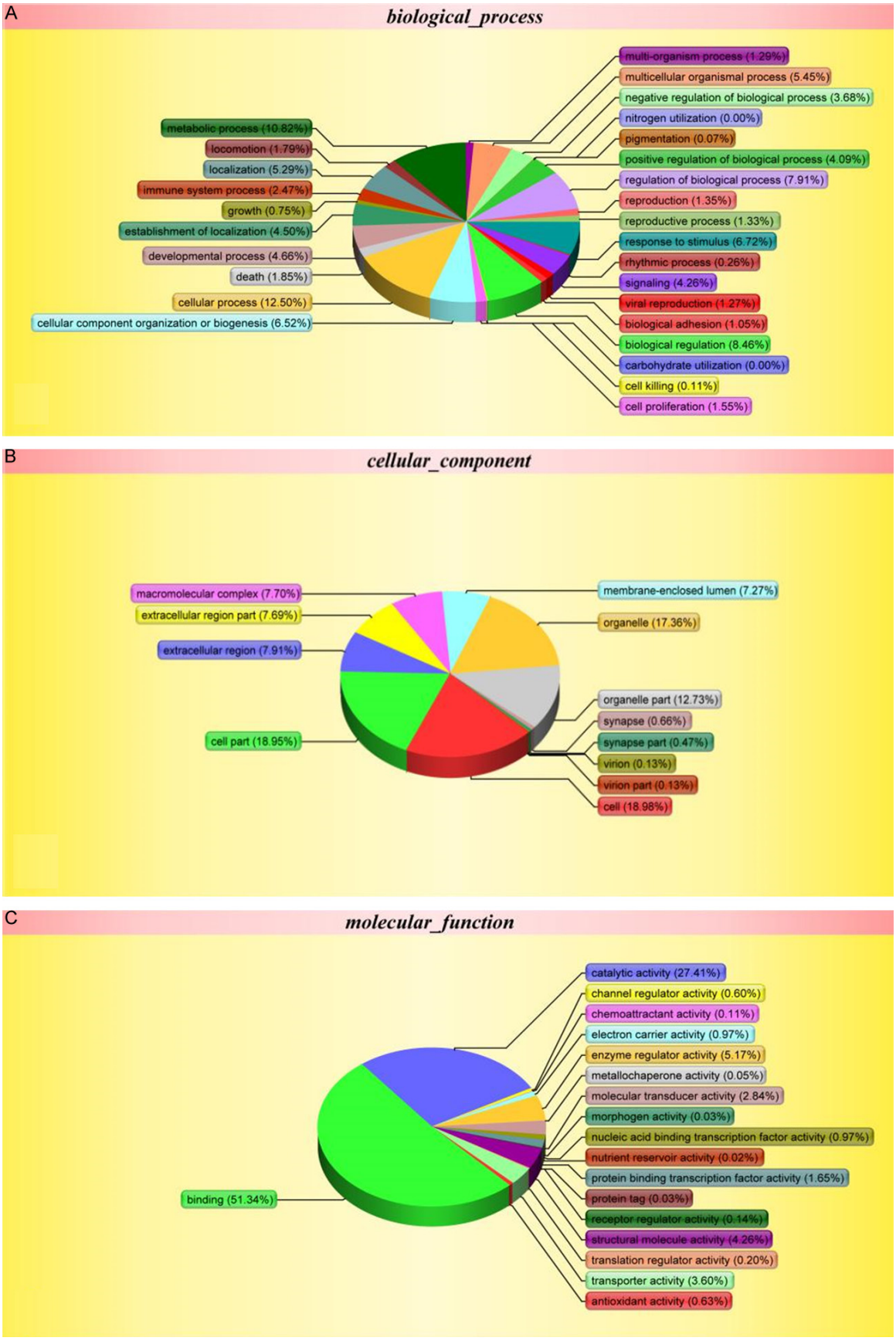

Figure 6. GO classification of all identified proteins. A. Biological process. B. Cellular component. C. Molecular function. GO, Gene Ontology.

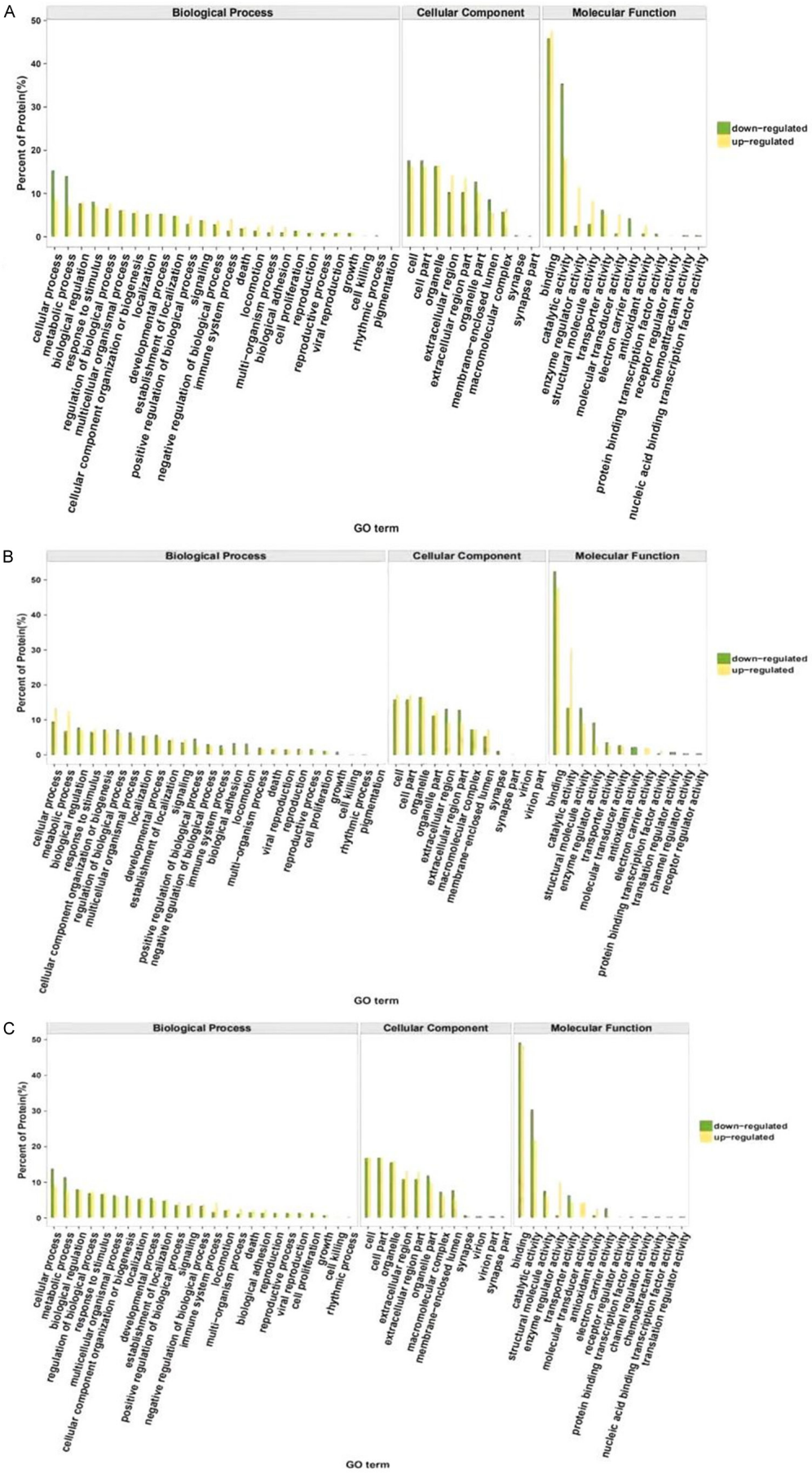
A
Biological Process
Cellular Component
Molecular Function
Percent of Protein(%)
down-regulated
up-regulated
GO term
B
Biological Process
Cellular Component
Molecular Function
Percent of Protein(%)
down-regulated
up-regulated
GO term
C
Biological Process
Cellular Component
Molecular Function
Percent of Protein(%)
down-regulated
up-regulated
GO term

Figure 7. GO classifications in Model vs Normal groups (A), Therapy vs Model groups (B), and Therapy vs Control groups (C) according to the biological processes (left), cellular component (middle), and molecular function (right). Green bar indicated the downregulated proteins, while yellow bar indicated the upregulated proteins. GO, Gene Ontology.

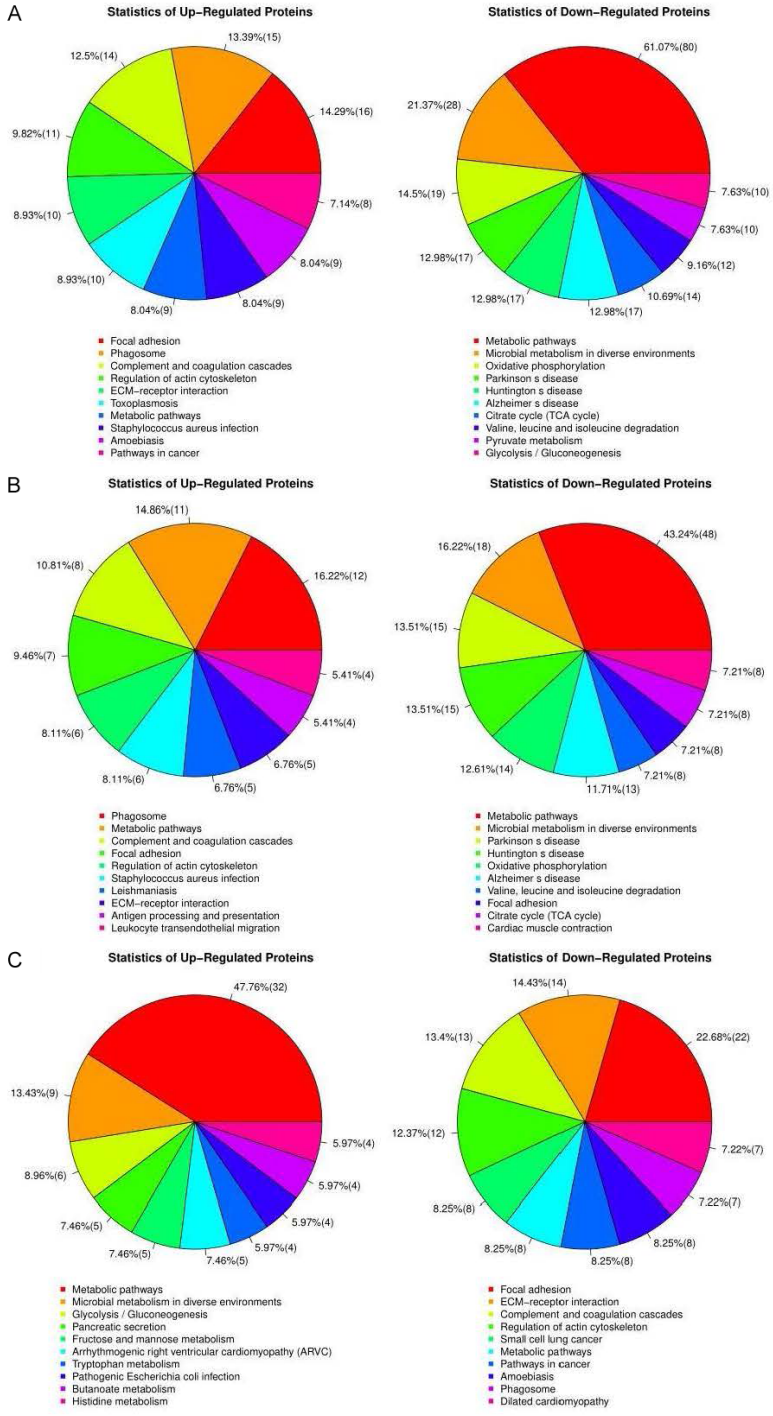

Figure 8. The top 10 pathways identified by KEGG in Model vs Normal groups (A), Therapy vs Model groups (B), and Therapy vs Normal groups (C). The number of proteins was marked in each bracket. KEGG, Kyoto Encyclopedia of Genes and Genomes.

nents, and 14 molecular functions (**Figure 7C**). Interestingly, we found noticeable differences in GO functional classification between the upregulated and downregulated proteins, as well as in the degree of functional concentration. For example, we found that more proteins involved in cellular process and metabolic process were upregulated in the DEPs of Normal vs Therapy groups. In contrast, more proteins related to immune system process and biological adhesion were downregulated.

Moreover, we utilized KEGG database to annotate protein pathways that were enriched to better understand the biological pathways and the molecular mechanisms underlying the disease development as well as identify vital biomarkers. The top 10 upregulated and downregulated proteins identified by KEGG analysis were shown in **Figure 8**, among which proteins in metabolic pathways were differentially expressed between the Normal and the Model groups but expressed oppositely between the Model and the Therapy groups. In addition, proteins involved in the two vital pathways, metabolic pathways, and focal adhesion, were both upregulated and downregulated, although more proteins in metabolic pathways were downregulated than upregulated.

KEGG pathway enrichment analysis can also identify the

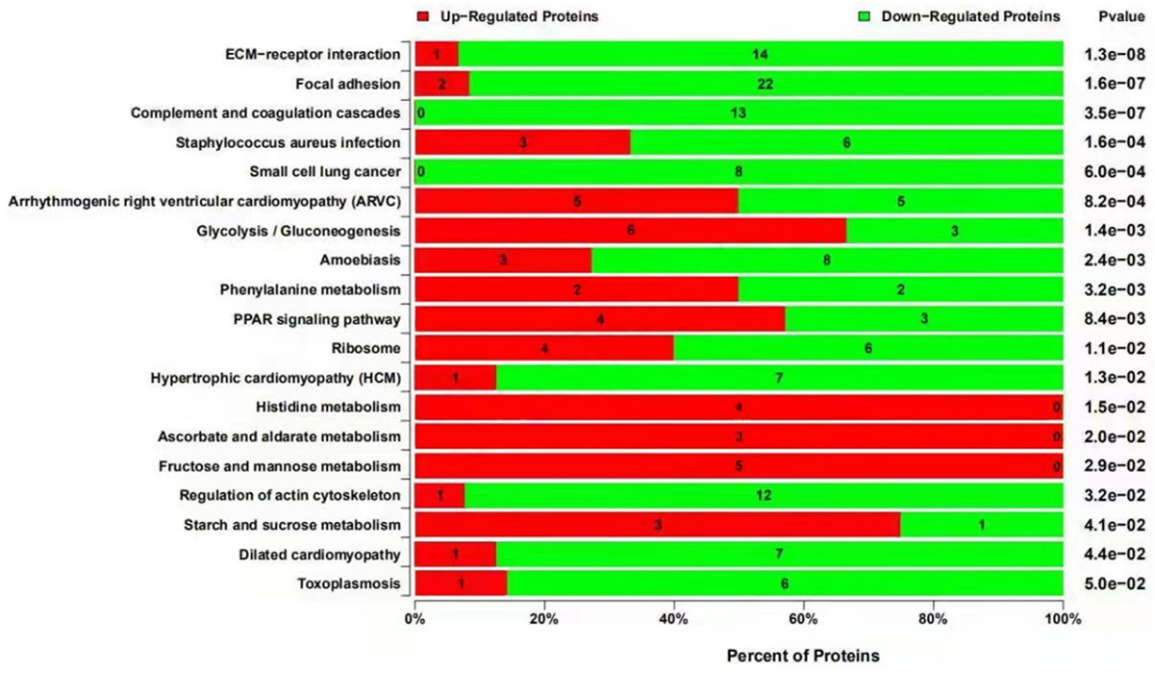

Figure 9. KEGG pathways in Therapy vs Model groups. Red represented the upregulated proteins, while green represented the downregulated proteins. KEGG, Kyoto Encyclopedia of Genes and Genomes.

Table 3. DEPs of complement and coagulation pathways in Model vs Therapy group

Protein ID	Protein name	Gene name	Ratio (Therapy/Model)	*P* value
P01027	Complement C3	C3	0.39	2.79776E-14
Q61838	Pregnancy zone protein	Pzp	0.33	1.17067E-09
Q3TGR2	Fibrinogen, B beta polypeptide	Fgb	0.32	1.6689E-08
Q3UEM7	Uncharacterized protein	Fgg	0.34	1.16714E-06
Q00897	Alpha-1-antitrypsin 1-4	Serpina1d	0.64	0.04788553
Q3V3W7	Uncharacterized protein	F13a1	0.46	0.000209702
E9PV24	Fibrinogen alpha chain	Fga	0.31	4.15811E-06
Q3UBS3	Haptoglobin	Hp	0.26	9.53067E-05
P06909	Complement factor H	Cfh	0.33	0.002255862
Q3V1T9	Plasminogen	Plg	0.64	0.027192229
Q00898	Alpha-1-antitrypsin 1-5	Serpina1e	0.26	0.01752943
B2RWX2	Complement component 4B	C4b	0.60	0.003675591
A0A0R4J038	Kininogen-1	Kng1	0.37	0.004141234

DEPs, differentially expressed proteins.

main biochemical metabolic pathways and signal transduction pathways that are enriched with DEPs. Our analysis showed that most of the DEPs between the Model and the Therapy groups was enriched in ECM-receptor interaction, focal adhesion, as well as complement and coagulation cascades (**Figure 9**). Strikingly, all DEPs involved in complement and coagulation cascades were downregulated by IMQ treatment (**Table 3**), suggesting that complement and coagulation cascades may play an important role in the function of IMQ in UC mice.

Discussion

UC is one of the main forms of inflammatory bowel disease (IBD), with clinical manifestations of abdominal pain, diarrhea, and hematochezia. If untreated, the alternating relapsing

and remitting mucosal inflammation can seriously impact patient quality of life [16]. Hence, safe and effective drugs are urgently needed.

IMQ, an agonist of TLR7, is a small molecule immunomodulatory compound that displays both antiviral and antitumor effects [17]. It has been demonstrated that IMQ can stimulate B cell proliferation by activating TLR7 [18]. In addition, Sainathan et al. have found that IMQ can induce type I IFN expression and increase the populations of dendritic cells (DC) in the gastrointestinal mucosa to ameliorate colitis [19]. Furthermore, a recent study has reported that IMQ is associated with the accumulation of Regulatory T cells (Tregs) during intestinal inflammation through the induction of CCR9 [20].

In this study, we used 3% DSS to induce acute colitis. Mice presented with diarrhea, hematochezia, and weight loss; all characteristics of clinical manifestations of UC. Importantly, we found that IMQ intervention could alleviate these clinical symptoms. In being consistent with our findings, IMQ has been previously reported to be effective in treating mice with UC by ameliorating the inflammatory response [19, 20]; however, little is known about its functional mechanism. Here, we used iTRAQ to analyze the DEPs among mice in different treatment groups and identified 4170 DEPs. Interestingly, we discovered a significant reduction in the levels of proteins that are involved in complement and coagulation cascades by the treatment of IMQ in KEGG pathway analysis, suggesting that complement and coagulation cascades might contribute to the therapeutic effect of IMQ in UC.

It has been known that overactivation of the complement system can lead to various diseases, although it plays an important role in eliminating bacteria, apoptotic cells, as well as malignant cells [21]. In addition, recent studies discover that the aberrant activation of the complement system not only leads to the pathogenesis of IBD but also contributes to the development of colitis-associated carcinogenesis by activating intestinal IL-1β/IL-17A axis [22].

From bioinformatics analysis, we found that the expression of complement C3, one of the most important complement components, was reduced by IMQ treatment. In agreement with our findings, a strong positive correlation between C3 and IL-17 mRNA expression in IBD has been reported, which can promote the production of pro-inflammatory cytokines (IL-17A, IL-6, TNF-α) [23]. In addition, another study has suggested that the complement components, such as C3, C4, and C1q, can effectively modulate the function of intestinal epithelial cells to induce intestinal stem cell proliferation and pro-inflammatory signaling activity [24]. Furthermore, TLR-4 mediated signals in intestinal epithelial cells can induce the expression of C3, leading to an increased production of pro-inflammatory to anti-inflammatory cytokines [25]. Consistent with these notions, reduction of C3, the central component of the complement system, has been reported to be protective against colitis [26]. Together, these findings suggest C3 is an important biochemical marker for the diagnosis and treatment of UC.

C4b, another vital component in the complement system, has a critical role in tissue clearance and microbial elimination. Recent studies have shown that the C4b gene number is positively correlated with inflammation in pediatric IBD. Additionally, C4b may be involved in the aberrant host reactivity to gut microbiota in children with IBD. Moreover, higher C4b gene copy number is associated higher fecal calprotectin level, which reflects higher intestinal inflammatory activity [27].

Plasminogen (Plg) can be converted into plasmin by the plasminogen activators (PAs). Interestingly, it has been reported that the expression of PAs is elevated in the patients with IBD [28]. The activation of plasmin and matrix metalloproteinases (MMPs) can break the intestinal epithelial barrier by degrading components of the extracellular matrix, thereby leading to the accumulation of inflammatory cells [29]. In fact, the expression of MMPs is upregulated in IBD and is associated with the severity of IBD [30]. In addition, Munakata et al. discovered that plasmin inhibition could prevent the progression of IBD in colitis models and attenuate inflammation by suppressing the MMP9-dependent influx of inflammatory cells and the production of inflammatory cytokines such as TNF-α [31]. Consistently, our results also showed that the expression of Plg was upregulated in DSS-treated mice, which was reversed by IMQ treatment. Hence, targeting

the expression of Plg may represent a novel therapeutic strategy for the treatment of colitis.

In this study, bioinformatics analysis found that C3, C4b and Plg were notably downregulated by IMQ treatment, suggesting that IMQ may regulate the complement and coagulation cascades. Thus, using inhibitors of the complement system may serve as an effective alternative to the current biological treatment of colitis.

Taken together, our findings indicate that the activation of the complement and coagulation cascades accelerates the inflammatory response during colitis procession, and inhibiting the expression of the proteins associated with complement and coagulation cascades could alleviate the inflammatory condition, which warrants further studies on the effects of IMQ in patients with UC and on the function of DEPs identified by iTRAQ.

Conclusions

IMQ may exert protective effects on mice with DSS-induced colitis through suppressing the activation of the complement and coagulation cascades. Targeting the complement and coagulation cascades may be an effective therapeutic strategy for the treatment of patients with UC.

Acknowledgements

The present study was supported by the Scientific and Technological Project of Hubei Province (grant No. 2015BKB013).

Disclosure of conflict of interest

None.

Address correspondence to: Dr. Zhongyin Zhou, Department of Gastroenterology, Renmin Hospital of Wuhan University, Hubei Key Laboratory of Digestive System Disease, 238 Jiefang Road, Wuhan 430060, Hubei, China. E-mail: zhongyinzhou@whu.edu.cn

References

[1] Segal JP, LeBlanc JF and Hart AL. Ulcerative colitis: an update. Clin Med (Lond) 2021; 21: 135-139.

[2] Du L and Ha C. Epidemiology and pathogenesis of ulcerative colitis. Gastroenterol Clin North Am 2020; 49: 643-654.

[3] Olén O, Erichsen R, Sachs MC, Pedersen L, Halfvarson J, Askling J, Ekbom A, Sørensen HT and Ludvigsson JF. Colorectal cancer in ulcerative colitis: a Scandinavian population-based cohort study. Lancet 2020; 395: 123-131.

[4] Porter RJ, Kalla R and Ho GT. Ulcerative colitis: recent advances in the understanding of disease pathogenesis. F1000Res 2020; 9: F1000 Faculty Rev-294.

[5] Calvino-Suarez C, Ferreiro-Iglesias R, Baston Rey I and Barreiro-de Acosta M. Managing ulcerative colitis after surgery. Front Med (Lausanne) 2023; 9: 1081940.

[6] Trutnovsky G, Reich O, Joura EA, Holter M, Ciresa-König A, Widschwendter A, Schauer C, Bogner G, Jan Z, Boandl A, Kalteis MS, Regauer S and Tamussino K. Topical imiquimod versus surgery for vulvar intraepithelial neoplasia: a multicentre, randomised, phase 3, non-inferiority trial. Lancet 2022; 399: 1790-1798.

[7] Gao J, Chen F, Fang H, Mi J, Qi Q and Yang M. Daphnetin inhibits proliferation and inflammatory response in human HaCaT keratinocytes and ameliorates imiquimod-induced psoriasis-like skin lesion in mice. Biol Res 2020; 53: 48.

[8] Chuang KC, Chang CR, Chang SH, Huang SW, Chuang SM, Li ZY, Wang ST, Kao JK, Chen YJ and Shieh JJ. Imiquimod-induced ROS production disrupts the balance of mitochondrial dynamics and increases mitophagy in skin cancer cells. J Dermatol Sci 2020; 98: 152-162.

[9] Baslam M, Kaneko K and Mitsui T. iTRAQ-based proteomic analysis of rice grains. Methods Mol Biol 2020; 2139: 405-414.

[10] Palstrøm NB, Matthiesen R and Beck HC. Data imputation in merged isobaric labeling-based relative quantification datasets. Methods Mol Biol 2020; 2051: 297-308.

[11] Husain I, Ahmad W, Ali A, Anwar L, Nuruddin SM, Ashraf K and Kamal MA. Functional neuroproteomics: an imperative approach for unravelling protein implicated complexities of brain. CNS Neurol Disord Drug Targets 2021; 20: 613-624.

[12] Xu HM, Huang HL, Liu YD, Zhu JQ, Zhou YL, Chen HT, Xu J, Zhao HL, Guo X, Shi W, Nie YQ and Zhou YJ. Selection strategy of dextran sulfate sodium-induced acute or chronic colitis mouse models based on gut microbial profile. BMC Microbiol 2021; 21: 279.

[13] Dieleman LA, Palmen MJ, Akol H, Bloemena E, Peña AS, Meuwissen SG and Van Rees EP. Chronic experimental colitis induced by dextran sulphate sodium (DSS) is characterized by Th1 and Th2 cytokines. Clin Exp Immunol 1998; 114: 385-391.

[14] Du M, Hou Z, Liu L, Xuan Y, Chen X, Fan L, Li Z and Xu B. Progress, applications, challenges and prospects of protein purification technology. Front Bioeng Biotechnol 2022; 10: 1028691.
[15] Karimi F, Hamidian Y, Behrouzifar F, Mostafazadeh R, Ghorbani-HasanSaraei A, Alizadeh M, Mortazavi SM, Janbazi M and Naderi Asrami P. An applicable method for extraction of whole seeds protein and its determination through Bradford's method. Food Chem Toxicol 2022; 164: 113053.
[16] Van Assche G, Peyrin-Biroulet L, Sturm A, Gisbert JP, Gaya DR, Bokemeyer B, Mantzaris GJ, Armuzzi A, Sebastian S, Lara N, Lynam M, Rojas-Farreras S, Fan T, Ding Q, Black CM and Kachroo S. Burden of disease and patient-reported outcomes in patients with moderate to severe ulcerative colitis in the last 12 monthsmulticenter European cohort study. Dig Liver Dis 2016; 48: 592-600.
[17] Frega G, Wu Q, Le Naour J, Vacchelli E, Galluzzi L, Kroemer G and Kepp O. Trial watch: experimental TLR7/TLR8 agonists for oncological indications. Oncoimmunology 2020; 9: 1796002.
[18] Hirobe S, Yamasaki T, Ito S, Quan YS, Kamiyama F, Tachibana M and Okada N. Transcutaneous administration of imiquimod promotes T and B cell differentiation into effector cells or plasma cells. Pharmaceutics 2022; 14: 385.
[19] Sainathan SK, Bishnupuri KS, Aden K, Luo Q, Houchen CW, Anant S and Dieckgraefe BK. Toll-like receptor-7 ligand imiquimod induces type I interferon and antimicrobial peptides to ameliorate dextran sodium sulfate-induced acute colitis. Inflamm Bowel Dis 2012; 18: 955-967.
[20] Chen L, Zhou Z, Yang Y, Chen N and Xiang H. Therapeutic effect of imiquimod on dextran sulfate sodium-induced ulcerative colitis in mice. PLoS One 2017; 12: e0186138.
[21] Gavriilaki E and Brodsky RA. Complementopathies and precision medicine. J Clin Invest 2020; 130: 2152-2163.
[22] Ning C, Li YY, Wang Y, Han GC, Wang RX, Xiao H, Li XY, Hou CM, Ma YF, Sheng DS, Shen BF, Feng JN, Guo RF, Li Y and Chen GJ. Complement activation promotes colitis-associated carcinogenesis through activating intestinal IL-1β/IL-17A axis. Mucosal Immunol 2015; 8: 1275-1284.
[23] Edwards JA, Tan N, Toussaint N, Ou P, Mueller C, Stanek A, Zinsou V, Roudnitsky S, Sagal M, Dresner L, Schwartzman A and Huan C. Role of regenerating islet-derived proteins in inflammatory bowel disease. World J Gastroenterol 2020; 26: 2702-2714.
[24] Sina C, Kemper C and Derer S. The intestinal complement system in inflammatory bowel disease: Shaping intestinal barrier function. Semin Immunol 2018; 37: 66-73.
[25] Li Y, Tang M, Zhang FJ, Huang Y, Zhang J, Li J, Wang Y, Yang J and Zhu S. Screening of ulcerative colitis biomarkers and potential pathways based on weighted gene co-expression network, machine learning and ceRNA hypothesis. Hereditas 2022; 159: 42.
[26] Abbasi N, Long T, Li Y, Yee BA, Cho BS, Hernandez JE, Ma E, Patel PR, Sahoo D, Sayed IM, Varki N, Das S, Ghosh P, Yeo GW and Huang WJM. DDX5 promotes oncogene C3 and FABP1 expressions and drives intestinal inflammation and tumorigenesis. Life Sci Alliance 2020; 3: e202000772.
[27] Dheer R, Davies JM, Quintero MA, Damas OM, Deshpande AR, Kerman DH, Sawyer WP, Pignac-Kobinger J, Ban Y, Fernandez I, Burgueno JF, Phillips MC and Abreu MT. Microbial signatures and innate immune gene expression in lamina propria phagocytes of inflammatory bowel disease patients. Cell Mol Gastroenterol Hepatol 2020; 9: 387-402.
[28] Kaiko GE, Chen F, Lai CW, Chiang IL, Perrigoue J, Stojmirović A, Li K, Muegge BD, Jain U, VanDussen KL, Goggins BJ, Keely S, Weaver J, Foster PS, Lawrence DA, Liu TC and Stappenbeck TS. PAI-1 augments mucosal damage in colitis. Sci Transl Med 2019; 11: eaat0852.
[29] He L, Kang Q, Chan KI, Zhang Y, Zhong Z and Tan W. The immunomodulatory role of matrix metalloproteinases in colitis-associated cancer. Front Immunol 2023; 13: 1093990.
[30] Lucafò M, Pugnetti L, Bramuzzo M, Curci D, Di Silvestre A, Marcuzzi A, Bergamo A, Martelossi S, Villanacci V, Bozzola A, Cadei M, De Iudicibus S, Decorti G and Stocco G. Long non-coding RNA GAS5 and intestinal MMP2 and MMP9 expression: a translational study in pediatric patients with IBD. Int J Mol Sci 2019; 20: 5280.
[31] Czajkowska A, Guzinska-Ustymowicz K, Pryczynicz A, Lebensztejn D and Daniluk U. Are matrix metalloproteinase-9 and tissue inhibitor of metalloproteinase-1 useful as markers in diagnostic management of children with newly diagnosed ulcerative colitis? J Clin Med 2022; 11: 2655.